

# Composite action in connection regions of concrete-filled steel tube columns

Mathias Johansson†

*Department of Structural Engineering, Concrete Structures, Chalmers University of Technology  
SE-412 96 Göteborg, Sweden*

(Received October 11, 2002, Accepted February 4, 2003)

**Abstract.** In a nonlinear finite element study on the mechanical behavior of simple beam connections to continuous concrete-filled steel tube columns, two principally different connection types were analyzed: one with plates attached to the outside of the tube wall, relying on shear transfer, and one with an extended plate inserted through the steel section to ensure bearing on the concrete core. The load was applied partly at the connection within the column length and partly at the top, representing the load from upper stories of a multi-story building. The primary focus was on the increased demand for load transfer to ensure composite action when concrete with higher compressive strength is used. The results obtained from the analyses showed that the design bond strength derived from push tests is very conservative, mainly due to the high frictional shear resistance offered by pinching and contraction effects caused by connection rotation. However, with higher concrete strength the demand for load transfer increases, and is hard to fulfill for higher loads when connections are attached only to the steel section. Instead, the connection should penetrate into the concrete core to distribute load to the concrete by direct bearing.

**Key words:** composite columns; concrete-filled steel tube; composite action; bond; connections; finite element analysis.

## 1. Introduction

The use of concrete-filled steel tube (CFT) columns in multi-story buildings, horizontally braced by shear walls, has increased around the world in recent years as the benefits of increased stiffness and load resistance for a reduced cross section, resulting in an increase in usable floor space, have been realized. These advantages can be enhanced further by the use of high-strength concrete (HSC). However, the structural benefits of CFT columns require load transfer between the steel tube and the concrete core to ensure their composite action. Especially for CFT columns filled with HSC, the need for high load transfer can be expected since the concrete core is supposed to carry an increased part of the total normal force.

Careful design of the top and bottom of a single-story high column or the connections of a continuous column is necessary to ensure that the loading is introduced to the composite cross section in a proper way. This means that loads should be transferred from the beams in such a way that all structural components of the column contribute to the load-bearing according to their strength. The load introduction is seldom a problem for the single-story column see Bergman (1994), Kilpatrick and Rangan (1999) and Johansson (2001) since the forces from the continuous beam can be transferred to

---

†M.Sc. and Lic. Sc., Research Assistant

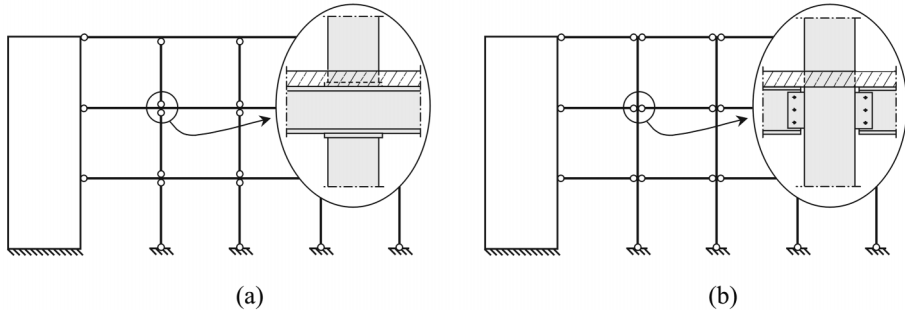


Fig. 1 (a) Single-story high columns with head-plates and (b) continuous columns with simple connections

the column by direct bearing on head-plates; see Fig. 1a.

However, for continuous columns the cheapest connections are achieved by attaching plates to the outside of the steel tube; see Fig. 1b. In this case, strain compatibility between the two materials is unlikely to be achieved, and the load transfer from the steel tube to the concrete core depends on the ability of the interface to resist shear stresses. Comprehensive studies on the bond strength for push tests have been reported in the literature; among many examples are those of Virdi and Dowling (1980), Roik *et al.* (1984), Shakir-Khalil (1991), Shakir-Khalil (1993a), Shakir-Khalil (1993b) and Roeder *et al.* (1999). Despite the large number of push tests available in the literature, they provide limited information about the real bond behavior in CFT columns. In addition, push tests do not always, if ever, represent the loading condition in an actual CFT column. Moreover, these connection regions are the places in a frame where the highest shear stress demand exists.

Far less work, though, has been done on the influence of bond in more realistic situations such as regions of load introductions and the load transfer mechanisms. This is still not well understood. In tests on simple beam-column connections by Dunberry *et al.* (1987), Shakir-Khalil (1992), Shakir-Khalil (1993b) and Shakir-Khalil (1994), it has been shown that the shear transfer resistance in the connection region could be considerably higher than that obtained from push tests, mainly explained by the pinching effect. In case of insufficient shear resistance, one way to increase the load transfer is to extend the loading plate through the steel section, which ensures that the concrete core is loaded by direct bearing; see Roik *et al.* (1988).

The purpose of this study was to examine the stress situation around simple beam connections to CFT columns more thoroughly, with the use of three-dimensional nonlinear finite element (FE) analyses. The primary focus was on the increased demand for load transfer to ensure composite action when concrete with higher compressive strength is used. Two principally different connections were studied: one with plates attached just to the outside of the steel tube, and one with an extended plate inserted through the steel section. The first relied on shear transfer and the second on direct bearing upon the concrete core. In the FE analyses, part of the load was applied to the simple beam connection within the column length; and part was applied to the top of the model, representing the load from upper stories of a multi-story building.

## 2. Composite action

### 2.1. Load distribution and redistribution

In the European Prestandard, Eurocode 4 (1992) (EC4), full composite action up to maximum load

resistance shall be assumed in the design of composite columns. Full composite action means strain compatibility between the steel section and the concrete section, and consequently no slip should occur in the interface between the concrete core and the steel tube. This requires that internal forces and moments applied to the column are distributed between the concrete core and the steel tube according to their response to the imposed deformations.

In the ultimate limit state, the distribution of the normal force may be calculated on the basis of plastic resistance of the cross section parts. The steel component part ( $N_{a,Sd}$ ) of the total normal force ( $N_{Sd}$ ), often called the steel contribution ratio  $\delta$ , can be determined for pure axial loads as

$$\delta = \frac{N_{a,Sd}}{N_{Sd}} = \frac{N_{pl,a,Rd}}{N_{pl,Rd}} = \frac{A_a f_y}{A_a f_y + A_c f_{co}} \quad (1)$$

where  $N_{pl,a,Rd}$  is the plastic resistance of the steel section,  $N_{pl,Rd}$  is the plastic resistance of the total cross section,  $A_a$  is the steel area,  $A_c$  is the concrete area,  $f_y$  is the yield strength of the steel and  $f_{co}$  is compressive strength of the concrete. Accordingly, the remaining part of the normal force has to be carried by the concrete ( $N_{c,Sd}$ ):

$$\frac{N_{c,Sd}}{N_{Sd}} = 1 - \delta \quad (2)$$

The distribution of the internal forces in the ultimate limit state does not necessarily coincide with the distribution in the serviceability limit state. For the latter, the distribution depends on the longitudinal stiffness. The steel component can be written as:

$$\frac{N_{a,Sd}}{N_{Sd}} = \frac{A_a E_a}{A_a E_a + A_c E_c} \quad (3)$$

and the concrete component as

$$\frac{N_{c,Sd}}{N_{Sd}} = 1 - \frac{N_{a,Sd}}{N_{Sd}} \quad (4)$$

where  $E_a$  and  $E_c$  are modulus of elasticity of the steel and the concrete respectively. If the concrete core is reinforced, the resistance of the reinforcement may be added to the concrete part.

In regions where concentrated loads are introduced to the column, it can be difficult to ensure that all cross-section parts of the composite column are loaded according to their resistance. Consequently, full composite action does not exist in these regions of the column, and to achieve this the load has to be redistributed, considering the shear resistance at the interface between the concrete and the steel. According to EC4, this shear resistance shall be provided by bond stresses and friction or by mechanical shear connectors, such that no significant slip occurs. Furthermore, the transfer (introduction) length,  $l_v$ , of the shear force should not be assumed to exceed twice the relevant transverse dimension; for CFT columns with circular section, this means twice the diameter of the column. Thus, if an external load is introduced only to the steel part, the component of the load given by Eq. (2) and Eq. (4) has to be transferred over the interface to the concrete core within the introduction length, for the ultimate state and serviceability limit state, respectively.

There is no well-established method for calculating the longitudinal shear stress at the interface. Therefore, design is usually based on the mean shear stress found by dividing the shear force by an

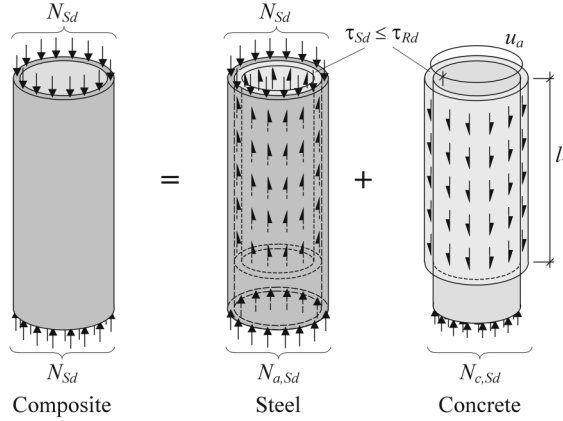


Fig. 2 Shear transfer between the steel tube and the concrete core

assumed shear transfer interface area. This area is given by the perimeter of the section,  $u_a$ , and the transfer length; see Fig. 2. The design shear stress is given by

$$\tau_{sd} = \frac{N_{c,Sd}}{u_a l_v} \quad (5)$$

where  $N_{c,Sd}$  is the design concrete force according to Eq. (2) or Eq. (4).

The maximum transferable shear stress,  $\tau_{sd}$ , must not exceed the design bond strength  $\tau_{rd}=0.4$  MPa. If the acting shear stress exceeds the admissible value, the load transfer has to be achieved by mechanical shear connectors. However, in CFT columns with smaller dimensions, it is of great practical and economic interest to omit any mechanical shear connectors at the interface between the concrete core and the steel tube.

With the use of HSC both the concrete compressive strength and the E-modulus of the concrete increase, and from Eqs. (1)-(4) it is obvious that this means that the concrete core takes an increased part of the total normal force, both in the serviceability limit state and the ultimate limit state. Hence, in connection regions, this requires that more shear force can be transferred over the interface. Moreover, redistribution of the forces from the concrete to the steel may take place due to long-term effects. In fact, the bond stress demand can be even greater in the serviceability limit state when long-term effects are present, than in the ultimate limit state; see Roik and Bode (1980). Creep can be taken into account by using a fictitious modulus of elasticity for the concrete in Eq. (3).

## 2.2. Shear transfer between the steel and the concrete

The design “bond strength” given in EC4 is based on push (or push-out) tests performed by Roik *et al.* (1984). It is defined as the average interface shear stress associated with the residual load due to friction. No adhesive bond is taken into account.

As in EC4, the behavior of shear transfer in the interface between the concrete and the steel in a composite column is often based on the experimental behavior obtained from push tests. These tests usually reveal a stiff initial part and a peak load that is highly dependent on the surface quality of the steel section. For additional deformation, the load decrease and finally a residual resistance due to frictional bond remain.

The initial bond is provided by adhesion between the steel and the concrete; see Fig. 3a. This is often termed chemical bond. It is an elastic brittle shear transfer mechanism that is active mainly at the early

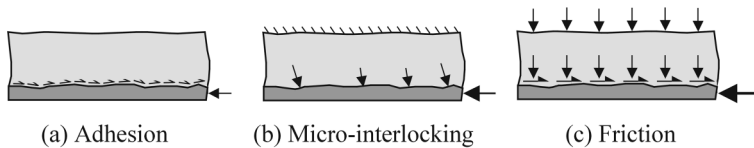


Fig. 3 Idealized shear transfer mechanisms in the steel-concrete interface

stage of loading when the relative displacements are small. Kennedy (1984) found that its contribution to transfer shear stresses can be neglected for composite columns since the adhesion stress is exceeded at a slip value less than 0.01 mm. Furthermore, the shrinkage of the concrete core has an adverse effect on the development of adhesion stresses.

With increasing shear, this adhesion resistance is exceeded, and the subsequent strength depends on the mechanical characteristics at the interface. Here, two features exist: the bond provided by the mechanical microlocking of the concrete and the steel, and the bond that depends on the interface pressure and the coefficient of friction; see Fig. 3b-c.

The microlocking relates to the surface roughness of the steel tube. According to Virdi and Dowling (1980), this bond breaks when the concrete interface attains a local strain of approximately 3.5% associated with the compressive crushing of concrete. They found that surface roughness increased the bond strength. This mechanism contributes to a typical initial stiff part of the load-deformation relationship obtained from tests.

Friction develops between the concrete core and the steel tube due to normal stresses, for instance caused by volumetric increase of the concrete core when subjected to compressive loading, or irregularities in the steel tube, often referred to as macrolocking. Although microlocking and friction apply to different scales, they are very closely related and can be regarded as the same type of phenomenon, and no separation between these two types of mechanical bond is further made in this paper.

It has been shown that the concrete compressive strength does not increase the “bond strength”. This is important since the need for shear transfer can be assumed to be higher with the use of HSC. It has also been argued whether and how the “bond strength” in CFT columns depends on: the sectional shape; dimensions ( $d/t$ ); length of steel-concrete interface; slenderness; and load eccentricities. For example, it has been shown that the average bond stress evaluated from push tests is greater in circular than in rectangular CFT columns. However, this is not explained by better bond strength; the differences refer to structural effects, i.e., the rigidity of the tube walls against pressure perpendicular to their plane. The magnitude of the shear stresses due to friction depends directly on the amount of normal stresses that can be built up. This effect can be seen in push tests on concrete-filled steel tubes carried out by Shakir-Khalil (1993a). He found that in a circular section the overall perimeter resisted the slip, while a rectangular section was effective in resistance only in the vicinity of the corners. Hence, the interface shear transfer due to mechanical bond is more pronounced for concrete-filled steel tubes with circular cross section than with rectangular cross section; but this is due to structural effects rather than higher bond strength between the concrete and the steel. Furthermore, the bond strength evaluated from push tests shows a large scatter, which is found to be directly related to the irregularities in the diameter and shape of the tubes; see Roeder *et al.* (1999). Again, this can be attributed to structural effects.

The deformation and stress situation obtained in push tests will never or at least rarely occur in an actual CFT column. However, it can be argued that the results from these tests are on the safe side, and are appropriate for use in design. Although this is perhaps true in most cases, there exist cases when it is not so, for instance, when the load is applied only to the steel section at the top of a CFT column. In this

case the steel tube expands outwards and almost no load is transferred to the concrete core and the CFT column acts more or less like an empty steel tube; see Johansson (2001). It illustrates the problem when studying the shear transfer mechanism in this simplified way by the use of design bond strength. It is important to realize that the bond stresses cannot be treated as a constant bond strength with uniform distribution. In reality the bond stresses will vary; local contact pressures can exist that are much higher than in the push tests, resulting in the possibility of high shear stresses due to friction without significant slip. This effect can be very apparent in regions around connections. The shear mechanisms should be studied more locally and the possibility to account for higher interface contact pressure should also be included. Baltay and Gjelsvik (1990) performed tests to determine the coefficient of friction between concrete and mild steel for a wide range of normal stresses: from 7 kPa to almost 490 MPa. The average coefficient of friction was found to be 0.47, which clearly shows the possibility to transmit high shear stresses in the steel-concrete interface.

### **3. Mechanical behavior of simple connections**

#### *3.1. Need for improvement*

From the discussion above, it is obvious that our knowledge about the true stress situation around simple connections to CFT columns has to increase in order to understand the load transfer and the interaction between the concrete core and the steel tube. The stresses in the load introduction area are determined by using either complete elastic design or full plastic design. Reality lies anywhere between these two methods and the real stress situation can be very complicated. To study the stress situation around connection regions more thoroughly, three-dimensional nonlinear FE models can be used. The use of finite element programs is perhaps not economical for practical engineers. However, only with increased knowledge is it possible to derive more realistic mechanical models that can be used in design, and hopefully also lead to more economical solutions.

#### *3.2. Finite element modeling*

##### *3.2.1. General remarks*

Few analytical studies have been conducted where the slip and stress transfer between the steel tube and the concrete core has been taken into account. Hajjar *et al.* (1998) presented a fiber-based distributed-plasticity FE approach for analysis of square and rectangular CFT columns. This model accounts for slip between the concrete and the steel by incorporation of a nonlinear slip interface. Although this model shows good correspondence with experimental results, it is hard to use in studies of local behavior. Its advantages lie especially in global frame analyses where the CFT columns are parts of a complete structure. A drawback is that constant values of the initial slip stiffness and bond strength are used over the entire interface of the column. As shown, the shear transfer is mainly accounted for by friction, thus depending on the contact pressure, which locally can be very high. If a local phenomenon is to be studied, these effects have to be taken into account. However, with increased knowledge about the load transfer mechanisms, this kind of global model can be further improved and form a very powerful tool in structural analyses where detailed 3D modeling is not possible.

The models used in this study are based on solid elements where the interface between the steel tube and the concrete core is simulated with a surface-based interaction using a Coulomb friction model.

The surfaces of the concrete and the steel can separate and slide relative to each other, as well as transmitting contact pressure and shear stresses. Furthermore, both material and geometric nonlinear behavior is taken into account, i.e. confinement effects, local buckling and second-order effects are considered. These are matters of vital importance if the real stress situation around connection detailing to CFT columns is being studied.

### *3.2.2. Modeling of the concrete, the steel and the interaction*

The concrete core was modeled using eight-node solid elements with reduced integration. For plain concrete a special material option called “concrete” is provided in ABAQUS; see HKS (2001). When the principal stress components are predominantly compressive, the response of the concrete is modeled by elastic-plastic theory. The elastic stress state is limited by a Drucker-Prager yield surface. Once yielding has occurred, an associated flow rule together with isotropic hardening is used. The uniaxial stress-strain relations in compression, used in the analyses, were determined in accordance with the CEB Bulletin d'Information 228 (1995). In tension, the model uses a smeared crack approach, which means that it does not track individual “macro” cracks. A crack is assumed to occur when the stresses reach a failure surface called the “crack detection surface.” Once cracking has appeared, a damage elasticity model describes the post-failure behavior of the concrete. Although the model should be able to treat the behavior of concrete in both compression and tension, a convergence problem occurred when plastic compressive strain and cracking were obtained in the same integration point. To overcome this problem, linear elasticity was assumed in tension. However, it was shown that compressive stresses dominated and only limited tensile stresses occurred in few locations. Accordingly, the tensile behavior of the concrete was of secondary importance in these analyses.

To model the steel in the tube and the connection details, eight-node solid elements with full integration were used. A bi-linear stress-strain relationship was used for all steel elements. It was assumed that all steel components behaved the same way in compression as in tension. An elastic-plastic model, with the von Mises yield criterion, associated flow rule and isotropic strain hardening, was used to describe the constitutive behavior of the steel; see HKS (2001).

The interfaces between the steel and the concrete were simulated with surface-based interaction by the use of gap elements available in ABAQUS; see HKS (2001). A hard contact pressure-overclosure model gives the contact pressure,  $p$ . When the surfaces are in contact, any contact pressure can be transmitted between them; if the surfaces separate, the pressure reduces to zero. In the basic form of the Coulomb friction model, two contacting surfaces can carry shear stresses across their interface up to a given magnitude before they start sliding relative to one another. The Coulomb friction model defines this critical shear stress,  $\tau_{crit}$ , at which frictional slip starts. The critical shear stress is proportional to the contact pressure between the surfaces ( $\tau_{crit} = \mu p$ ), where  $\mu$  is known as the coefficient of friction. It is also possible to specify an upper limit,  $\tau_{max}$ , on the critical shear stress. The behavior remains elastic as long as the shear stress does not exceed the critical stress.

### *3.3. Modeling of experiments from literature*

As was described in Section 2.2, the majority of the experiments that have been conducted to determine the behavior of the shear transfer in the interface between the concrete core and the steel tube have been push tests with focus on the bond strength. However, some tests have been carried out to study the more realistic shear transfer and slip around simple connections to CFT columns. Shakir-Khalil (1993b) performed modified push tests, where short CFT specimens were provided with

200 mm high brackets through which the load applied to the concrete core was transferred to the supports; see Fig. 4a. The compressive strength of the concrete was  $f_{co} = 40.1$  MPa and the steel had a yield strength of  $f_y = 318$  MPa and a modulus of elasticity of  $E_a = 208$  GPa.

The length of the steel-concrete interface was 400 mm. He concluded that circular sections were much more effective than rectangular sections in resisting push forces. The specimen D1 with circular section supported a load in excess of 800 kN and the failure was due to the failure of the brackets, which were not designed to support such high loads. The obtained load resistance is approximately 10 times the predicted resistance given by assuming the design bond strength ( $\tau_{Rd} = 0.4$  MPa) over the entire steel-concrete interface. Furthermore, interestingly, only very small slip takes place even at high load levels. The load-slip relationship obtained by the FE analysis was very sensitive to the value of the coefficient of friction that was used, and a value of 0.5 gave the best agreement with the experimental results; see Fig. 4b. By the use of FE analysis it can be concluded that the high resistance is mainly attributable to the pinching mechanism. In Fig. 5a, it can clearly be seen how the bracket has rotated and a separation between the steel tube and the concrete core has taken place over most of the bracket height. Despite this separation, it can be seen that the pinching effect is more than adequate to compensate for the loss of bond in the tensile zone of the bracket, and the main load is transferred over the interface by friction in a small area at the lower part of the bracket, where very high contact pressure occurs; see Fig. 5c.

The maximum shear stress obtained in the FE analysis was 31 MPa. After opening of the specimen, Shakir-Khalil (1993b) found clear pressure points on the concrete core at the same locations where high contact pressure was obtained in the FE analysis. But shear stresses also occur in the upper part of the bracket where contact pressure develops due to contraction of the steel tube; see Fig. 5c. This shows that the load transfer mechanism in a connection region can be very different from that in push tests and that it is possible to transmit high shear stresses if the friction mechanism is taken into account. However, this test is rather extreme and, as in push tests, such a stress situation probably will not occur in a real CFT column.

Nonetheless, the same author also performed tests on more realistic simple beam-column connections; see Shakir-Khalil (1992). The specimens consisted of CFT columns with the same cross section dimensions as above and a length of 2.8 m, with steel beams bolted to the column through the use of 360 mm high

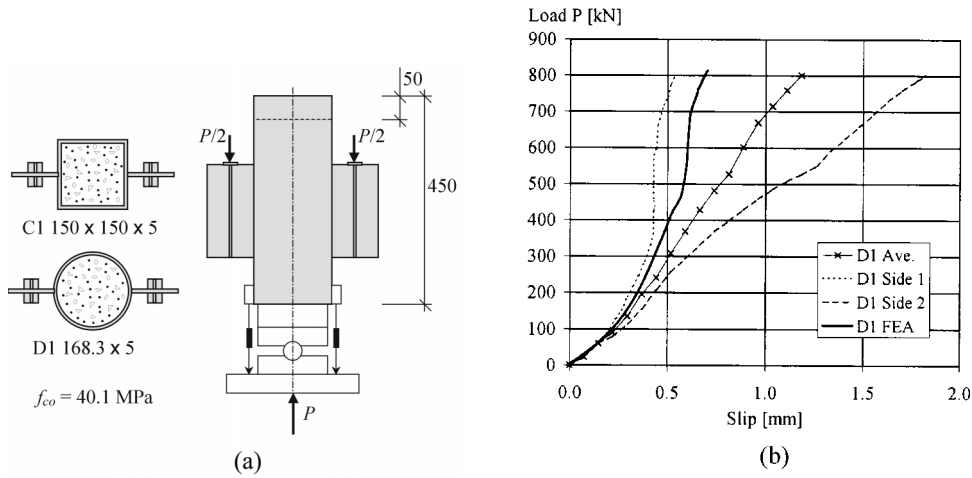


Fig. 4 (a) Test setup and (b) load-slip relation for specimen D1

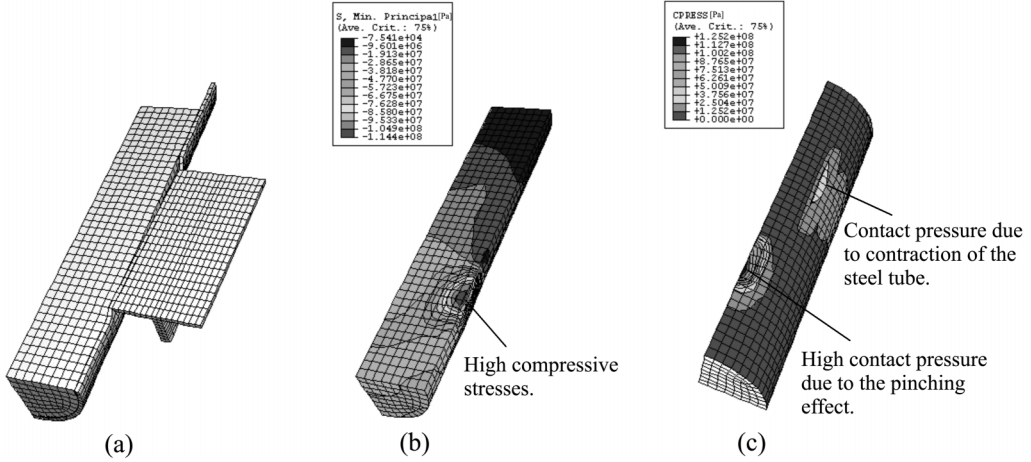


Fig. 5 Results from the FE analysis: (a) deformed shape, (b) minimum principal stress (in Pa) in the concrete core and (c) contact pressure (in Pa) at the concrete core

plates welded to the wall of the steel tube; see Fig. 6a. Both the column and the beams were loaded to represent a column in a multi-story building. For specimen A6, used here as comparison, the beams were loaded symmetrically, and the loads were applied at a distance of 250 mm from the face of the column, i.e., the load eccentricity of the column was  $e = 334$  mm. The beam and the column loads,  $P_2$  and  $P_1$ , were increased proportionately with the ratio 1:5. Accordingly, the total applied load is:  $P = P_1 + 2P_2$ . The compressive strength of the concrete was  $f_{co} = 34.8$  MPa and the steel had a yield strength of  $f_y = 318$  MPa and a modulus of elasticity of  $E_a = 208$  GPa.

The coefficient of friction value 0.5 that was calibrated for specimen D1 was also used in the established FE model of specimen A6. The maximum load resistance predicted by the FE analysis was 1447 kN, which is in good correspondence with the failure load of 1421 kN that was obtained in the test. Fig. 6b shows measured longitudinal strains in the steel at three different load levels, i.e. 250, 500 and 1000 kN, versus the height of the column for the experiment and FE analysis. The FE model matches the experimental strain measurements fairly well for these load levels. The distribution of the axial force between the concrete core ( $N_c$ ) and the steel tube ( $N_a$ ) is shown in Fig. 6c for the same three load levels as in the strain comparison. As can be seen, the load transfer is completed well within the distance of two times the diameter ( $2D$ ) below the connection.

The shear load transfer behavior is very similar to that shown for specimen D1. However, the load transfer due to the pinching effect at the lower part of the plate is not as dominant as for specimen D1. Instead, the effect of contraction of the steel tube in the part subjected to high lateral tensile stresses also has a great influence on the load transfer, especially at higher load levels; see Fig. 7. The first yielding in the steel tube occurs in the upper part of the connection, due to the biaxial stress state caused by longitudinal compressive stresses from the load  $P_1$  and the lateral tensile stresses from the rotation of the connection. However, the maximum load resistance is limited by yielding in the steel section below the plates. As for specimen D1, the concrete is subjected to very high local stresses in the lower part of the plate. These are distributed very quickly and the total plastic resistance of the concrete section ( $N_{pl,c,Rd} = A_c f_{co}$ ) is never reached.

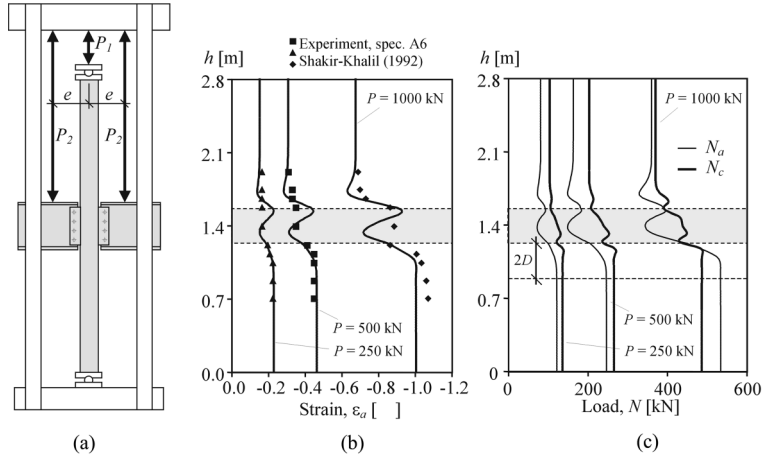


Fig. 6 (a) Test set-up of specimen A6, (b) comparison between test and FE analysis of axial strains in the steel tube, and (c) distribution of the axial force between the concrete core ( $N_c$ ) and the steel tube ( $N_a$ ) obtained from FE analysis

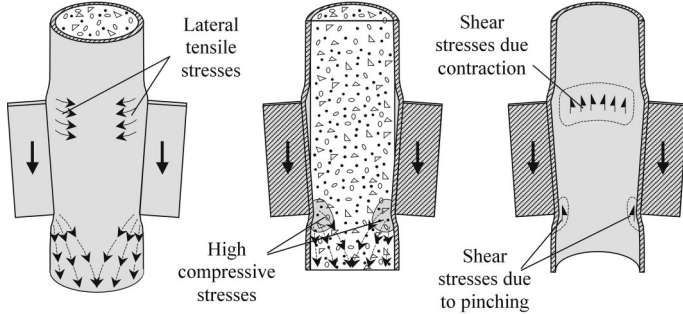


Fig. 7 Pinching and contraction effects due to connection rotation

### 3.4. Numerical study of simple connections

#### 3.4.1. Model description

To study the mechanisms of load transfer, and the influence of concrete compressive strength and interface conditions, a numerical study was performed. It was in principle the same FE model as used in the comparison in Section 3.3. However, the load application, load ratio, material properties and the geometry of the column were slightly changed. The outer diameter of the steel tube was 160 mm and the wall thickness was 5 mm. A steel yield strength of  $f_y = 350$  MPa and a modulus of elasticity of  $E_a = 200$  GPa were used. To study the influence of different resistance of the concrete core, five concrete compressive strengths,  $f_{co}$ , were used: 40, 60, 80, 100 and 120 MPa. The corresponding modulus of elasticity,  $E_c$ , was calculated from the compressive strength according to CEB Bulletin d'Information 228 (1995) as

$$E_c = E_{co} (f_{co}/f_{cmo})^{0.3} [\text{GPa}] \quad (6)$$

where  $E_{co} = 22$  GPa and  $f_{cmo} = 10$  MPa. This expression is valid for both high-strength and normal-

strength concrete.

To minimize the influence of the boundary conditions on the behavior of load transfer in the connection region, half the height of the column above and below the connection was modeled, corresponding to a total height of 2.8 m. The concrete core and the steel tube are restrained to each other at the top and the bottom of the FE model, since it is assumed that strain compatibility is obtained in these locations in the continuous column. The beams were not modeled; instead, the beam loads were applied directly through the boltholes in the plates, at a distance of 70 mm from the face of the column, corresponding to the shear force that could be expected in a simple connection. The height of the plates was 150 mm and the thickness was 10 mm. A higher steel grade, with higher yield strength (500 MPa) and modulus of elasticity (210 GPa), was assumed for the plates. Furthermore, for simplicity, the welds were assumed to be strong enough not to influence the resistance and were therefore not modeled. The column was loaded symmetrically; therefore, only  $\frac{1}{4}$  of the column section was modeled. In practice there will always be load eccentricities and slenderness effects present, but according to Roeder *et al.* (1999) these effects increase the shear transfer resistance due to binding effects. Therefore, it is on the safe side if the connection is able to distribute the load to the concrete core and the steel tube under the extreme condition of axial loading.

The column was loaded to represent an internal column in a multi-story building of 10 floors above

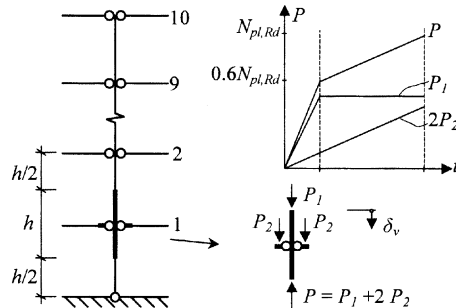


Fig. 8 The loading sequence of the column

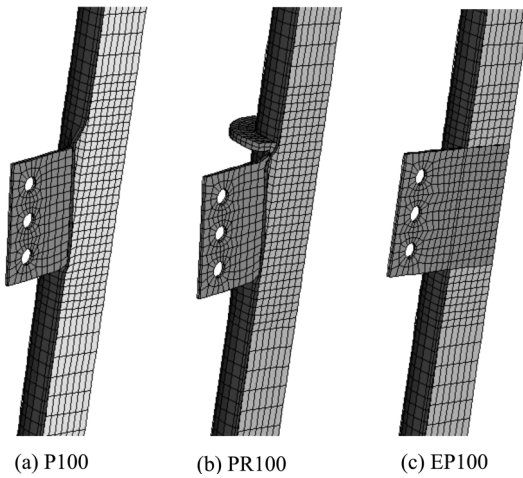


Fig. 9 Deformed shape at maximum load,  $P_{\max}$

the ground floor. The plate and column loads,  $P_2$  and  $P_1$ , were increased proportionately with the ratio 1:18 up to 60% of the column ultimate section strength ( $N_{pl,Rd} = A_{afy} + A_{fcu}$ ); see Fig. 8.

Then, to simulate overload at the first floor, the column load ( $P_1$ ) was kept constant and the plate load ( $P_2$ ) was increased until the maximum load resistance was obtained. Since the resistances between the columns in this study were different, the evaluation of the columns was more consistent with this loading sequence. In principle, two different connection types were studied: one with plates (denoted P) attached just to the outside of the steel wall, and one with an extended plate (denoted EP) inserted through the steel section; see Fig. 9. The former was also studied when it was strengthened with a stiffening ring above the plate (denoted PR).

To investigate the maximum resistance of the different connection types for a column filled with a concrete compressive strength of 100 MPa, some analyses were also performed with load applied only to the plates ( $P_1 = 0$ ). Here, two cases were studied: firstly, when the tube and the core were restrained at the top of the model (marked "r"), secondly, when they were unrestrained (marked "u") and consequently were permitted to slip relative to each other. A summary of all performed analyses in the numerical study can be seen in Table 1.

### 3.4.2. Results and discussion

In Fig. 10, the load-deformation relationships for the connection types P and EP, with different concrete strengths, are compared. The load  $P$  is the total force in the section at mid-height of the ground floor, i.e. the bottom of the FE model. The deformation,  $\delta_s$ , is the vertical top deformation of the FE model; see Fig. 8. For clarity, the origin for eight of the curves has been shifted horizontally along the deformation axis; however, in all cases, the deformation at zero load is zero.

The pronounced change in the curves after the first, almost linear part corresponds to 60% of the calculated ultimate resistance, where the loading is changed. Before this point, there is no visible difference between the connection types. This is not surprising since most of the total load originates from the load from the stories above ( $P_1$ ) that has already been distributed according to the response of the section. The differences can be seen in the second part of the loading, where the load from the beams ( $P_2$ ) should be transferred to the column. For the lowest concrete strength, there is almost no difference between the connection types P and EP; however, with increasing concrete strength, the difference becomes more apparent. The stiffness and the load resistances are lower for the connection type P compared with the connection type EP for the same concrete strength. The load resistance,  $P_{max}$ , for connection type EP is in no case lower than 90% of the calculated maximum load resistance of the section ( $N_{pl,Rd}$ ). However, the load resistance for the connection type P falls to 83% for the highest concrete strength; see Table 1.

It is interesting to note that the difference in load distribution between the concrete core and the steel tube does not vary much. In fact, for all cases the yield strength of the entire steel section is obtained below the plate. The difference is thus the ability of the connection to transfer load to the concrete core. For all cases, the load transfer was completed within the distance of  $2D$  below the plates. The distribution of the total applied load, between the concrete core and the steel tube, at a distance of  $2D$  below the plate is shown in Fig. 11. As can be seen, the distributions obtained in the FE analyses correspond rather well with the expected distributions, for both the ultimate limit state (us) and the serviceability limit state (ss), according to Eqs. (1)-(4) described in section 2.1. The distribution in the serviceability limit state is taken at the load  $0.6N_{pl,Rd}$ , where the response of the materials is assumed to be elastic, and in the ultimate limit state at the maximum load resistance ( $P_{max}$ ). Important to notice, as discussed in Section 2.1, is that the need for load transfer in the connection region increases when

Table 1 Summary of the numerical study

Analysis	$f_{co}$ [MPa]	$E_c$ [GPa]	$\mu$	Restr.	$N_{pl,Rd}$ [kN]	$P_{\max}$ [kN]	$P_{\max} / N_{pl,Rd}$	$N_{c,P2}$ [kN]	$N_{c,Sd} / N_{Sd}$ (Eq. 2)	$N_c / P_{\max}$ (us)	$N_{c,Sd} / N_{Sd}$ (Eq. 4)	$N_c / 0.6 N_{pl,Rd}$ (ss)
Load on the plates and on the column top												
P40	40	33.3	0.5	yes	1559	1517	0.97	226	0.45	0.45	0.55	0.49
P60	60	37.7	0.5	yes	1912	1813	0.95	372	0.55	0.53	0.58	0.56
P80	80	41.1	0.5	yes	2266	2084	0.92	509	0.62	0.60	0.60	0.58
P100	100	43.9	0.5	yes	2619	2277	0.87	594	0.68	0.64	0.61	0.60
P120	120	46.4	0.5	yes	2973	2469	0.83	674	0.71	0.68	0.63	0.60
EP40	40	33.3	0.5	yes	1559	1507	0.97	222	0.45	0.45	0.55	0.51
EP60	60	37.7	0.5	yes	1912	1829	0.96	387	0.55	0.54	0.58	0.57
EP80	80	41.1	0.5	yes	2266	2118	0.93	538	0.62	0.60	0.60	0.59
EP100	100	43.9	0.5	yes	2619	2424	0.93	706	0.68	0.65	0.61	0.61
EP120	120	46.4	0.5	yes	2973	2662	0.90	813	0.71	0.68	0.63	0.61
P100 $\mu 0$	100	43.9	0.0	yes	2619	2237	0.85	602	0.68	0.66	0.61	0.57
P100 $\mu 02$	100	43.9	0.2	yes	2619	2265	0.86	622	0.68	0.66	0.61	0.59
EP100 $\mu 0$	100	43.9	0.0	yes	2619	2384	0.91	668	0.68	0.64	0.61	0.61
PR100	100	43.9	0.5	yes	2619	2321	0.89	655	0.68	0.66	0.61	0.60
PR100 $\mu 0$	100	43.9	0.0	yes	2619	2274	0.87	678	0.68	0.68	0.61	0.58
Load only on the plates ( $P_1 = 0$ )												
P100r	100	43.9	0.5	yes	2619	864	0.33	507	0.68	0.59	-	-
P100u	100	43.9	0.5	no	2619	864	0.33	463	0.68	0.54	-	-
P100 $\mu 02r$	100	43.9	0.2	yes	2619	855	0.33	431	0.68	0.50	-	-
P100 $\mu 02u$	100	43.9	0.2	no	2619	851	0.32	214	0.68	0.25	-	-
P100 $\mu 0r$	100	43.9	0.5	yes	2619	835	0.32	283	0.68	0.34	-	-
P100 $\mu 0u$	100	43.9	0.0	no	2619	814	0.31	18	0.68	0.02	-	-
EP100u	100	43.9	0.5	no	2619	1060	0.40	596	0.68	0.54	-	-
EP100 $\mu 0u$	100	43.9	0.0	no	2619	1058	0.40	630	0.68	0.60	-	-
PR100u	100	43.9	0.5	no	2619	911	0.35	448	0.68	0.49	-	-
PR100 $\mu 0u$	100	43.9	0.0	no	2619	857	0.33	25	0.68	0.03	-	-

concrete with higher compressive strength is used; hence, the demand on the connection performance increases. The amount of the total beam load ( $2P_2$ ) that is carried by the concrete core,  $N_{c,P2}$ , corresponds to the load that has been transferred from plates to the core; see Table 1.

As expected, the behavior of the connection type P is very similar to that of specimen A6 described in Section 3.3. The shear transfer at lower load levels is dominated by the pinching effect at the lower part of the plate. The first yielding in the steel tube occurs in the upper part of the plate, which leads to an increased rotation of the connection and increases the distortion of the tube wall. Then, localized yielding starts to develop below the plate when the steel tube is overstressed. This causes some slip at the interface and additional load at the plate is taken by tension in the steel tube above the connection and then transferred into the concrete core mainly by shear stresses offered by the contraction effect; see Fig. 7. The maximum load transfer in accordance with EC4 would be 56.5 kN, assuming the design bond strength over a transfer length

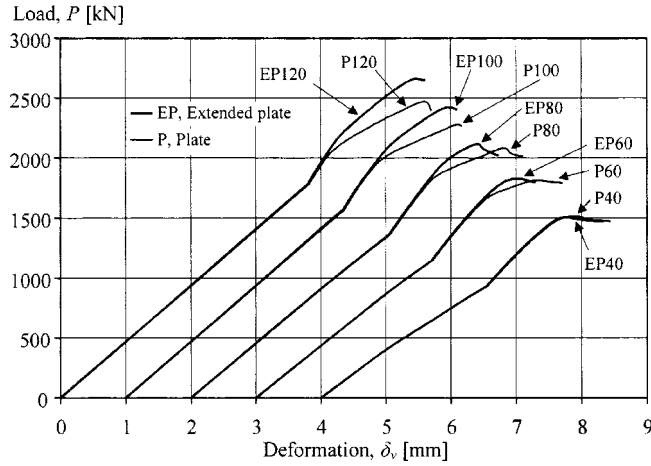


Fig. 10 Load-deformation relations for the connection types P and EP, with different concrete strength

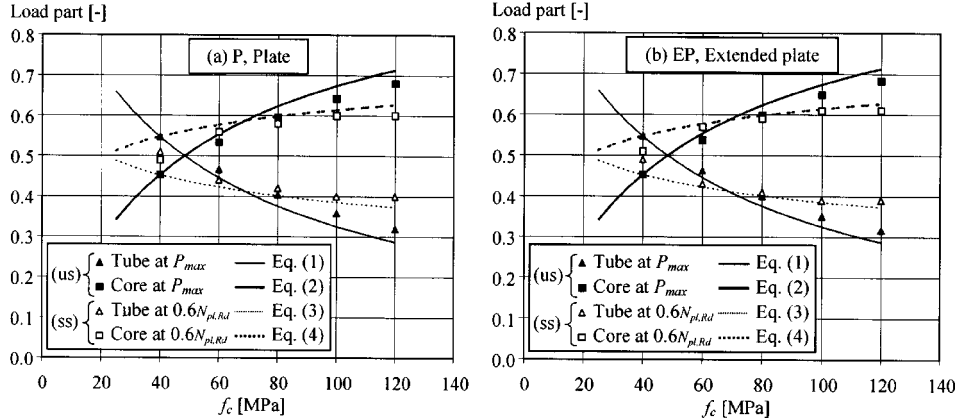


Fig. 11 Comparison of the expected distribution from Eqs. (1)-(4) and that obtained 2D below the connection in the FE analyses

of 2D. This is evidently very conservative when it is compared with the transfer load ( $N_{c,P2}$ ) obtained in the FE analyses; see Table 1. This conservatism was indicated earlier, although even more interestingly, when the bond strength is reduced, the resulting effect is larger deformations but not a drastic reduction in load resistance as could be expected; see Table 1 and compare P100 and P100 μ0 in Fig. 12.

Furthermore, how is it possible that the concrete core carries approximately the same amount of the beam load also with lack of bond strength, as for P100 μ0 (See Table 1.) Apparently, friction cannot be the only load transfer mechanism causing redistribution of load. One possible answer can be found in the results from the analyses of the connection type P loaded only at the plates ( $P_1 = 0$ ). For the exceptional case of no bond at the interface and no restraint between the tube and the core at the top (P100 μ0u), the steel tube becomes overstressed earlier and, since no load can be transferred to the core, the behavior is approximately as it would be for an empty steel column, except that the core delays potential local buckling. However, if the core and the tube are restrained at the top (P100 μ0r), load from the connection will be taken by tension in the tube to the top, transferred into the concrete core and down to the support by compression. This behavior was also recognized in tests performed by

Dunberry *et al.* (1987), where rectangular CFT columns were loaded through plates. The top of the columns was either provided with a steel cap plate welded to the steel tube or left without any plate, corresponding to the restrained and unrestrained cases respectively.

In reality, there will always exist some bond that can redistribute load from the tube to the core and, as can be observed in Table 1 for P100u and P100  $\mu$ 02u, the transferred load ( $N_{c,P2}$ ) increases rapidly with increasing coefficient of friction. However, when these cases are compared with the corresponding restrained cases (P100r and P100  $\mu$ 02r), it is clear that part of the transferred load can still be attributed to the "restraint" effect at the top. In a real continuous CFT column, this restraint effect corresponds to a column splice plate. However, it will not exist for the intermediate connections and, even if the load transfer would probably be secured by an extended transfer zone, there will not be strain compatibility. Consequently, the assumption of full composite action will be violated in these transfer zones. Yet these observations regarding the transfer zone are on the safe side, because the condition in the FE model is very ideal compared to reality and, as discussed earlier, there will always exist macro locking due to binding effects and nonuniformity of the steel tube, which increases the shear transfer resistance.

The rotation of the plates in the connection type P causes large unwanted distortions of the tube wall, which can induce local buckling; see Fig. 9. Furthermore, the high lateral tensile stresses in the steel tube above the connection reduce the axial resistance of the steel tube, and the load from the stories above ( $P_1$ ) is redistributed to the concrete core. The distortions and lateral stresses can be somewhat reduced by the use of a stiffening ring above the plate (PR), and thereby some increase in stiffness and load resistance is obtained. However, the general behavior will still be the same as for the connection type P; see Fig. 12.

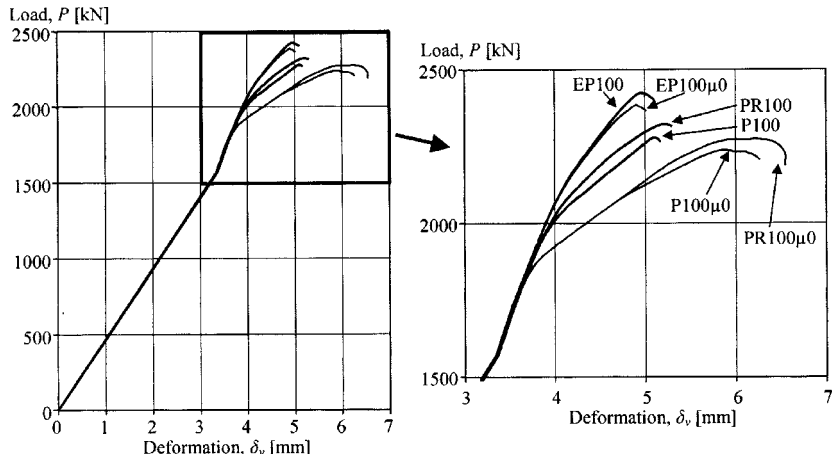


Fig. 12 Load-deformation relations for the connection types EP, P and PR, with different interface conditions, i.e. coefficient of friction 0.5 or 0

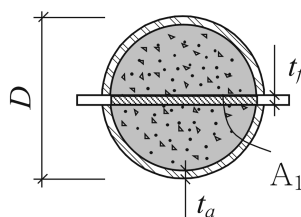


Fig. 13 Area of high local concrete stresses below the inserted plate

The load transfer mechanism for the connection type EP is, in contrast to the connection type P, rather simple. Since the plate is inserted through the steel section, it ensures that the concrete core is loaded by direct bearing. The concrete stresses below the plate can reach very high values, because the steel tube confines the concrete; see Fig. 13.

A design proposal for this type of load introduction was derived for normal-strength concrete based on tests by Roik *et al.* (1988) and is included in the design guide by CIDECT; see Bergman *et al.* (1995). The average concrete compressive stress below the plate should not exceed the value

$$f_{u1,Rd} = (f_{ck} + 35) \frac{1}{\gamma_c} \sqrt{\frac{A_c}{A_1}} \quad (7)$$

$$f_{u1,Rd} \leq \frac{N_{pl,c,Rd}}{A_1} \quad \text{and} \quad \frac{A_c}{A_1} \leq 20 \quad (8)$$

where  $A_c$  is the total concrete area,  $A_1$  is the area below the plate,  $f_{ck}$  is the characteristic concrete compressive strength,  $\gamma_c$  is the material safety factor for concrete and  $N_{pl,c,Rd}$  is the plastic resistance of the concrete core. These expressions should be valid for axial as well as eccentric loads. Moreover, in tests performed by Bergman (1994), it was indicated that this design proposal is applicable also for high-strength concrete. The assumed uniform distribution of the compressive stress below the plate is of course a simplification, and it was found in the FE analyses that the highest stresses occurred in the region close to the tube wall and decreased somewhat towards the middle of the plate. However, it is interesting to see that the level of the stresses ( $f_{u1,Rd}$ ) according to Eqs. (7) and (8) corresponds rather well with the stresses from the FE analyses, which were obtained by dividing the transferred load by the area below the plate ( $\sigma_{c1} = N_{c,P2} / A_1$ ); see Table 2. Here, the mean value of the compressive strength was used and the safety factor was taken as 1.0 in Eqs. (7) and (8).

The load transfer by shear stresses at the interface is of minor importance, as is obvious when EP100 μ0u and EP100u are compared. Although EP100 μ0u has no bond strength, it has a load resistance almost identical to that of EP100u and, in fact, even more load is transferred to the concrete core in the former; see Table 1. Furthermore, the inserted plate does not cause large distortions of the steel tube; see Fig. 9c.

To conclude, the main difference between the connection types P and EP is what happens after localized yielding occurs in the steel section below the plate. For the connection type P, further loading of the plates causes slip at the interface and additional load has to be taken by tension in the steel tube above the connection, and then gradually be transferred into the concrete core. For the connection type EP, slip between the steel tube and the concrete core is prevented due to the blocking action provided by the inserted plate, and the load is directly transferred to the concrete core. As a consequence of the

Table 2 Comparison of numerically obtained and calculated concrete stresses below the loading plate

Analysis	$f_{co}$ [MPa]	$f_{u1,Rd}$ [MPa]	$f_{u1,Rd} / f_{co}$	$N_{c,P2}$ [kN]	$\sigma_{c1}$ [MPa]	$\sigma_{c1} / f_{u1,Rd}$
EP40	40	257	6.4	222	148	0.57
EP60	60	326	5.4	387	258	0.79
EP80	80	395	4.9	538	359	0.91
EP100	100	463	4.6	706	471	1.02
EP120	120	532	4.4	813	542	1.02

different mechanical behavior, the stiffness is lower for the P compared with the EP when the yield strength for the steel tube is reached, as was observed for P60, P80, P100 and P120; see Fig. 10. Furthermore, this explains why the interface condition is of vital importance for the behavior of the P, and hardly at all influences the behavior of the connection type EP; see Fig. 12.

#### 4. Conclusions

The results obtained from the FE analyses on simple beam connections to concrete-filled steel tube columns, presented in this paper together with findings in referred literature, allow the following conclusions to be drawn. Both the connection type with plates attached only to the outside of the tube wall, and that with extended plate inserted through the steel section, were able to transfer high loads to the concrete core. In both cases the distribution of the internal normal force, between the concrete core and the steel tube, corresponds rather well with the expected distributions in the serviceability limit state and the ultimate limit state, assuming elastic and plastic response respectively. However, when concrete with higher compressive strength is used, the concrete core should take an increased part of the total normal force and the needs for load transfer in the connection region increase; hence, the demand on the connection performance increases. In the case of plates attached only to the steel section, this can cause problems with slip at the interface and unwanted distortions of the steel tube wall due to localized yielding and connection rotation.

The design bond strength for CFT columns given in EC4 has proved to be very conservative for the case of plates attached only to the outside of the steel tube. This is because the design bond strength is derived from push tests, which do not represent the deformation and stress situation in the connection region. The evidently higher shear transfer resistance can mainly be attributed to the high frictional shear stresses caused by the pinching and contraction effects. To derive more realistic mechanical models that can be used in design, although not the aim of this limited work, requires more analytical as well as experimental research.

Meanwhile, connection detailing attached only to the steel section have to be avoided for higher load levels, unless more advanced analysis methods are used to predict the real behavior of the connection region especially for higher concrete strengths where the need for higher shear load transfer can be expected. Instead, the connection should also penetrate into the concrete core to distribute load to the concrete by direct bearing. Here, shear transfer resistance at the interface is of minor importance and very high local compressive stresses can be allowed in the concrete below the bearing area, because of the confinement offered by the steel tube.

#### Acknowledgements

The author conducted the work presented in this paper as part of his Ph.D. studies at Chalmers University of Technology. The author wishes to thank his advisors, Professor Kent Gylltoft, Head of the Department of Structural Engineering, and Christina Claeson-Jonsson, Ph.D., NCC AB. The author wishes to express his gratitude to the Swedish Council for Building Research (BFR) (since 2001, FORMAS), the Development Fund of the Swedish Construction Industry (SBUF) and the construction company NCC AB, for financially supporting this project.

## References

- Baltay, P. and Gjelsvik, A. (1990), "Coefficient of friction for steel on concrete at high normal stress", *Journal of Materials in Civil Engineering*, **2**(1), Feb., 46-49.
- Bergman, R. (1994), "Load introduction in composite columns filled with high strength concrete", *Proceedings of the 6<sup>th</sup> International Symposium on Tubular Structures*, Monash University, Melbourne, Australia, 373-380.
- Bergman, R., Matsui, C., Meinsma, C. and Dutta, D. (1995), *Design Guide for Concrete Filled Hollow Section Columns under Static and Seismic Loading*, CIDECT series "Construction with hollow steel sections", Verlag TÜV Rheinland, Köln, Germany.
- CEB Bulletin d'Information 228 (1995), *High Performance Concrete, Recommended Extensions to the Model Code 90*, Research Needs. Lausanne, Switzerland, July.
- Dunberry, E., Leblanc, D. and Redwood, R. G. (1987), "Cross-section strength of concrete-filled HSS columns at simple beam connections", *Canadian Journal of Civil Engineering*, **14**, 408-417.
- European Prestandard, Eurocode 4 (1992), *Design of composite steel and concrete structures, Part 1-1: General rules and rules for buildings*. Ref. No.1994-1-1:1992, October.
- Hajjar, J. F., Schiller, P. H. and Molodan, A. (1998), "A distributed plasticity model for concrete-filled steel tube beam-columns with interlayer slip", *Engineering Structures*, **20**(8), Aug., 663-676.
- HKS (2001), *ABAQUS/Standard User's Manual, version 6.2*, Hibbit, Karlsson & Sorensen, Inc., Pawtucket, USA.
- Johansson, M. and Gylltoft, K. (2001), "Structural behavior of slender circular steel-concrete composite columns under various means of load application", *Steel and Composite Structures*, **1**(4), Dec., Techno-Press, 393-410.
- Kennedy, S. J. (1984), "End connection effects on the strength of concrete filled HSS beam columns", M.Sc. Thesis, Department of Civil Engineering, Edmonton, Alberta, Canada.
- Kilpatrick, A. E. and Rangan, B. V. (1999), "Influence of interfacial shear transfer on behavior of concrete-filled steel tubular columns", *ACI Structural Journal*, July-Aug., Title no. 96-S72, 642-648.
- Roeder, C. W., Cameron, B. and Brown, C. B. (1999), "Composite action in concrete filled tubes", *Journal of Structural Engineering*, **125**(5), May, 477-484.
- Roik, K. and Bode, B. (1980), "Composite action in composite columns", Sfintesco Festschrift, Paris, France, 287-302.
- Roik, K., Breit, M. and Schwalbenhofer, K. (1984), *Untersuchung der Verbundwirkung zwischen Stahlprofil und Beton bei Stützenkonstruktionen*, Studiengesellschaft für Anwendungstechnik von Eisen und Stahl e.V., Düsseldorf, Germany.
- Roik, K. and Schwalbenhofer, K. (1988), Experimentelle Untersuchung zum plastischen Verhalten von Verbundstützen, Bericht zu P125, Düsseldorf, Germany.
- Shakir-Khalil, H. (1991), "Bond strength in hollow concrete-filled steel hollow sections", *Proceedings, International Conference on Steel and Aluminium Structures, Composite Steel Structures*, Singapore, 157-168.
- Shakir-Khalil, H. (1992), "Full-scale tests on composite connections", *Composite Construction in Steel and Concrete II, Proceedings of the Engineering Foundation Conference*, Potosi, Missouri, June 14-19, ASCE, New York, USA, 539-554.
- Shakir-Khalil, H. (1993a), "Pushout strength of concrete-filled steel hollow sections", *The Structural Engineer*, **71**(13), 230-233 and 243.
- Shakir-Khalil, H. (1993b), "Resistance of concrete-filled steel hollow tubes to pushout forces", *The Structural Engineer*, **71**(13), 234-243.
- Shakir-Khalil, H. (1994), "Beam connections to concrete-filled tubes", *Proceedings of the 6<sup>th</sup> International Symposium on Tubular Structures*, Monash University, Melbourne, Australia, 357-364.
- Virdi, K.S. and Dowling, P.J. (1980), "Bond strength in concrete filled steel tubes", *IABSE Proceedings P-33/80*, Zürich, Switzerland, August, 125-139.